Journal of proteome research

Cite This: J. Proteome Res. XXXX, XXX, XXX−XXX

Article

pubs.acs.org/jpr

Quantitative Subcellular Proteomics of the Orbitofrontal Cortex of Schizophrenia Patients

Erika Velásquez,[†] Daniel Martins-de-Souza,[‡,§,¶] Ingrid Velásquez,[∥] Gabriel Reis Alves Carneiro,[⊥] Andrea Schmitt,[#] Peter Falkai,[#] Gilberto B. Domont,*[,†] and Fabio C. S. Nogueira*[,†,⊥]

[†]Proteomics Unit, Department of Biochemistry, Institute of Chemistry, Federal University of Rio de Janeiro, Rio de Janeiro 21941-909, Brazil

[‡]Laboratory of Neuroproteomics, Department of Biochemistry, Institute of Biology, University of Campinas (UNICAMP), Campinas 13083-970, Brazil

[§]Experimental Medicine Research Cluster (EMRC)University of Campinas, Campinas 13083-887, SP, Brazil

[¶]Instituto Nacional de Biomarcadores em Neuropsiquiatria (INBION), Conselho Nacional de Desenvolvimento Científico e Tecnológico (CNPq), São Paulo, Brazil

[∥]University of Carabobo, Naguanagua, Carabobo 2005, Venezuela

[⊥]Laboratory of Proteomics, LADETEC, Institute of Chemistry, Federal University of Rio de Janeiro, Rio de Janeiro 21941-598, Brazil

[#]Department of Psychiatry and Psychotherapy, Ludwig Maximilian University of Munich (LMU), 80539 Munich, Germany

Supporting Information

ABSTRACT: Schizophrenia is a chronic disease characterized by the impairment of mental functions with a marked social dysfunction. A quantitative proteomic approach using iTRAQ labeling and SRM, applied to the characterization of mitochondria (MIT), crude nuclear fraction (NUC), and cytoplasm (CYT), can allow the observation of dynamic changes in cell compartments providing valuable insights concerning schizophrenia physiopathology. Mass spectrometry analyses of the orbitofrontal cortex from 12 schizophrenia patients and 8 healthy controls identified 655 protein groups in the MIT fraction, 1500 in NUC, and 1591 in CYT. We found 166 groups of proteins dysregulated among all enriched cellular fractions. Through the quantitative proteomic analysis, we detect as the main biological pathways those related to calcium and glutamate imbalance, cell signaling disruption of CREB activation, axon guidance, and proteins involved in the activation of NF-kB signaling along with the increase of complement protein C3. Based on our data analysis, we suggest the activation of NF-kB as a possible pathway that links the deregulation of glutamate, calcium, apoptosis, and the activation of the immune system in schizophrenia patients. All MS data are available in the ProteomeXchange Repository under the identifier PXD015356 and PXD014350.

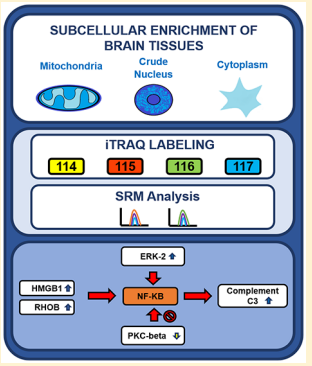

KEYWORDS: *schizophrenia, cellular fractions, proteomics, quantification*

1. INTRODUCTION

Schizophrenia is a chronic disease characterized by the impairment of mental functions with a marked social dysfunction. Over the years, several hypotheses have emerged about its etiology and physiopathology, but it is widely accepted that factors such as genetic susceptibility and environmental influences can cause the onset of the disease.[1] Diagnosis and classification depend mainly upon a collection of clinical features through the observation of positive symptoms including delusions, hallucinations, speech, or disorganized behavior as well as negative symptoms as affective bottling, anhedonia, alogia, avolition, social withdrawal, and impaired cognitive capacity.[2] Negative and cognitive symptoms currently remain without totally effective therapeutic options, persisting in the chronic phase.[3]

One of the main brain areas related to cognitive and behavioral disturbances is the frontal cortex. The dysfunction of this brain region is associated with mental disorders like psychosis, depression, and anxiety.[4] Particularly the orbitofrontal cortex (OFC), a subdivision of the prefrontal cortex, is involved in the emotional and executive processing, reward-guided behavior, and decision-making duet to its connection with neuroanatomical structures as the hippocampus, ventral striatum, amygdala, hypothalamus, anterior cingulate, and other medial temporal areas.[5] Clinical findings have linked social functioning impairment with anatomic structural

Special Issue: Human Proteome Project 2019

Received: June 16, 2019
Published: October 4, 2019

DOI: 10.1021/acs.jproteome.9b00398
J. Proteome Res. XXXX, XXX, XXX−XXX

abnormalities in the OFC in first-episode schizophrenia patients.[6] In the same way, it was shown that the relationship between structural brain abnormalities in the OFC and the severity of negative symptoms[7,8] suggest the key role of OFC in the abnormal emotional responses and social disability.

According to the Schizophrenia Working Group of the Psychiatric Consortium of Genomic (2014),[9] single nucleotide polymorphisms related to schizophrenia gene risk are associated with several genes involving dopamine receptor, glutamate neurotransmission, and immunity. Otherwise, transcriptomic data show that pathways linked with mitochondrial function and energy production, tight junction signaling, protein translation, neurodevelopment, and immune system seem to be very important in the pathophysiology of schizophrenia.[10−12]

Several studies have been carried out the proteomic characterization of post-mortem brain tissue of different areas from patients with schizophrenia, showing that the dysregulation of synaptic function as the NMDA receptors hypofunction, calcium homeostasis, imbalance of mitochondrial energy metabolism and oxidative stress, dysregulation in proteins of the cytoskeleton, and immune system are the main pathways reported so far.[13] However, only a few of these proteomic studies have deepened into the subcellular level.[14−16] The traditional proteomic approach lacks the important spatial information on the data; protein function is related to its environment, and the pathophysiological process can involve changes in protein subcellular localization.[17]

We analyzed OFC post-mortem brain tissue from patients classified as residual schizophrenia according to the DMS-IV manual. In this classification, the patients do not manifest prominent positive psychotic symptoms but prevail characteristic disturbance of negative symptoms.[18] Through the comparison of patient samples against a pool of control subjects without any history of psychiatric illness, we generated an organellar proteome map from different subcellular fractions such as mitochondria (MIT), crude nuclear fraction (NUC), and cytoplasm (CYT) with the aim to monitor the subproteome changes using iTRAQ labeling for relative quantification and selected reaction monitoring (SRM) for targeted quantification. Subcellular proteome maps allowed to observe dynamic changes in cell compartments providing valuable insights concerning schizophrenia physiopathology in the chronic phase of the disease.

2. EXPERIMENTAL PROCEDURES

2.1. Brain Samples

The OFC post-mortem tissues were collected from 12 schizophrenia patients at the State Mental Hospital in Wiesloch, Germany. Patients were diagnosed as residual schizophrenia (295.6) according to the Diagnostic and Statistical Manual of Mental Disorders (DSM-IV) criteria.[18] The OFC control samples were collected from eight individuals at the Institute of Neuropathology, Heidelberg University, in Heidelberg, Germany (Table S-1). It was selected control subjects without any medical records of mental clinical diseases, antidepressants, or antipsychotics treatment during their lifetime and no history of alcohol or drug abuse. Other neuropathologies were ruled out by histopathological analysis, considering only brains with Braak staging less than II. All assessments, post-mortem evaluations, and procedures were approved by the ethics committee of the Faculty of Medicine, Heidelberg University, Heidelberg, Germany.

2.2. Subcellular Enrichment

For nuclear enrichment, 50 mg of OFC tissue were homogenized in 10 volumes of Buffer A pH 7.4 (0.32 M sucrose, 4 mM HEPES, and protease cocktail inhibitor tablets (Roche)) and phosphatase inhibitor cocktails I and II (Sigma). The homogenate was centrifuged at 1 000*g* for 10 min, 4 °C obtaining the P1: crude nuclei. In the case of the mitochondria and cytoplasm enrichment, 30 mg of intact OFC brain tissue was incubated for 15 min on ice with 180 μL of 250-STM buffer (250 mM sucrose, 50 mM Tris-HCl pH 7.4, 5 mM $MgCl_2$, Mini protease inhibitor, and phosphatase inhibitor (Roche)). The tissue homogenization was made two times with a pestle for 1−2 min incubating for 10 min. The sample was centrifugated at 800*g* for 15 min 4 °C, obtaining the supernatant Cyt 1 (cytoplasm + mitochondria). The pellet was resuspended in 640 μL of 250-STM buffer, centrifuging at 800*g*, 15 min, 4 °C until the supernatant was clear. All supernatants were combined and centrifugated at 6 000*g*, 15 min, 4 °C. The last supernatant was collected as CYT fraction and saved to −80 °C until its use and the pellet (PM) was used for mitochondria enrichment.

PM was resuspended in 250 μL of 250-STM buffer and centrifuged at 6 000*g*, 15 min, 4 °C. The pellet was resuspended in 250 μL of Hepes buffer (10 mM Hepes, (pH 7.9/Mini protease inhibitor and phosphatase inhibitor (Roche) and incubated at 4 °C for 30 min (Eppendorf ThermoMixer, cold room/mixing). The enriched mitochondria were loaded on a sucrose gradient containing 1.75 mL of 50% sucrose, 1.75 mL of 36% sucrose, and 0.75 mL of 20% sucrose centrifuging at 25 000 rpm, 4 °C, 60 min. The MIT fraction was transferred to a new tube, filling in with Hepes buffer until 2 mL, and centrifuged at 17 200*g*, 20 min, 4 °C. This procedure was repeated four times. Finally, the pellet was stored at −80 °C until use.

2.3. Protein Extraction and Western Blot Analysis

Protein extraction was made according to the Saia-Cereda and collaborators protocol (2016),[15] determining the protein concentration by the Bradford assay (BioRad; Munich, Germany). SDS-PAGE electrophoresis and the Western blot analysis were previously described.[16] The Western blot image has been published in our previous study,[16] where the subcellular enrichment efficiency was evaluated using antibodies against collapsin 2 for cytosolic proteins, ATP synthase subunit alpha (ATP5A1) for mitochondrial proteins, postsynaptic density protein 95 (PSD95) for synaptosomal proteins, and histone deacetylase 1 (HDAC1) for nuclear proteins.[16]

2.4. Protein Digestion

Enzymatic digestion for iTRAQ labeling experiment used 10 μg of protein from MIT (n = 6), 25 μg of NUC (n = 12), 50 μg of CYT (n = 11), and control pool (20 μg of MIT, 100 μg of NUC, and 200 μg of CYT, all with n = 8). The samples were reduced with 5 mM TCEP for 1 h at 30 °C, alkylated with 10 mM iodoacetamide for 30 min at room temperature followed by dilution (1:10) with 50 mM triethylammonium bicarbonate (TEAB) pH 8 and digestion with trypsin (1:50) for 18 h at 35 °C. The samples were cleaned in C_{18}MacroSpin Columns (Harvard Apparatus). The peptides were dried in a Speed Vac and resuspended in 30 μL of TEAB 20 mM for Qubit assay

DOI: 10.1021/acs.jproteome.9b00398
J. Proteome Res. XXXX, XXX, XXX−XXX

quantification. For the SRM experiments, 8 μg of proteins from all subcellular fractions (MIT, n = 12; NUC, n = 8; and CYT, n = 12) and 8 μg of the control pool (n = 8 for MIT, NUC, and CYT) were digested following the procedure above.

2.5. Isobaric Tag Labeling with iTRAQ and Strong Cation Exchange (SCX)

The peptides from each subcellular fraction were labeled according to the Núñez and collaborators protocol (2017). The organization of 4-plex iTRAQ in all subcellular fractions was made up as follows: three channels (114, 115, and 116) were labeled with patients' samples and one channel (117) containing the pool of 8 control samples. Labeled peptides were dried to a volume of 20 μL. For SCX chromatography (MacroSpin Columns, Harvard Apparatus), the samples were completed to a final volume of 100 μL with a solution of KH_2PO_4 5 mM/ACN 25% pH 3. Peptides were eluted by one step with 500 mM KCl for MIT and NUC fractions and 75, 150, 250, and 500 mM KCl for the CYT fraction. Samples were desalted in C_{18}MacroSpin columns (Harvard Apparatus), dried, and suspended in 0.1% formic acid for quantification (Qubit Protein Assay Kit, Thermo Scientific).

2.6. Mass Spectrometry Analyses

Peptides (2 μg) were analyzed in technical triplicate by nLC Proxeon EASY-II system (Thermo Scientific). The chromatographic conditions were as follows: flow-rate of 250 nL/min, 3 h of gradient beginning with 5−40% B for 167 min, 40−95% B for 5 min, 95% B for 8 min, using as solvent A a solution of 95% H_2O/5% ACN/0.1% formic acid and solvent B 95% ACN/5% H_2O/0.1% formic acid. The analytical column length was 15 cm and an internal diameter of 75 μm (3 μm spheres, Reprosil Pur C18, Dr. Maish), and the trap-column length was 3 cm with an internal diameter of 200 μm (5 μm spheres, Reprosil Pur C18, Dr. Maish). Data acquisition was carried out under a stream atmosphere provided by 5% ammonium hydroxide.[19]

The chromatographic system was coupled online to an LTQ Orbitrap Velos (Thermo Scientific) mass spectrometer. A dynamic exclusion list of 90 s, spray voltage at 2.5 kV, and no auxiliary gas flow were the settings used for data-dependent acquisition mode. For Full MS scan, a scan range of m/z 375−2000 and a resolution of 60 000 (at m/z 400) was used in the Orbitrap analyzer. We selected the 10 most intense ions for fragmentation, excluding unassigned and the 1+ charge state, acquiring the MS^2 spectra in the Orbitrap (resolution of 7 500 at m/z 400) with higher-energy collision dissociation (HCD) using a normalized collision energy of 40.

2.7. Mass Spectra Analysis

Raw data were analyzed using Proteome Discoverer 2.1 software against the human database from neXtProt (February 12, 2019) using a target-decoy strategy (maximum delta CN of 0.05) and a false discovery rate (FDR) of 0.01. The search space was full-tryptic considering two missed cleavages. The precursor mass tolerance and fragment mass tolerance were 10 ppm and 0.1 Da, respectively. Fixed modification was included in the carbamidomethylation of cysteine. Methionine oxidation, protein N-terminal acetylation, and iTRAQ modifications (K, Y, and N-terminal) were considered as dynamic modifications. The peptide filter was set up for high confidence counting only peptides rank 1 with a minimum length of 6 amino acids and using as peptide validation settings an automatic control level peptide error with a strict target FDR of 0.01. The confidence threshold in the FDR protein validator was 0.01, grouping the proteins by maximum parsimony.

iTRAQ quantification was made with a unique peptide using the patients' value as a nominator and pool of controls as the denominator for fold-change calculations . Additional filters as a correction for the impurity reporter and a filter to not report quantitative values for a single-peak in the precursor isotope pattern were applied.

2.8. Statistical Evaluation of the Data

Data analyses were performed in the *InfernoRDN* program[20] using unique peptides. For data normalization, the Central Tendency and the absolute deviation of the adjusted median were applied. The Grubbs test, with a minimum of three peptides and p-value <0.05, was used as a parameter to group the peptides in their corresponding protein. Robust estimators, such as the median and median absolute deviation, were used to calculate the z-score and the p-value associated with a 95% confidence level, determining the statistically significant variations in the relative abundance of proteins. Also, *InfernoRDN* was used for the principal component analysis (PCA) of the different subcellular fractions.

2.9. Biological and Functional Analysis

Subcellular localization protein assignment was made using UniProt.[21] Comparative analyses of data were performed in the Venny 2.1 program.[22] The biological function was analyzed by Reactome Pathways[23] together with the STRING 10.5 software[24] (considering high-confidence interactions) and the KEGG program.[25]

2.10. SRM Analysis

The SRM analysis was performed in an EASYII-nano-LC (ThermoScientific) using a C18 column PicoChip 75 μm × 105 mm (New Objective) and C18 trap column Acclaim PepMap 75 μm × 2 cm (ThermoScientific). As solvent A was used a solution of 95% H_2O/5% ACN/0.1% formic acid and solvent B 95% ACN/5% H_2O/0.1% formic acid in a flow-rate of 320 nL/min during 60 min.

The data were acquired in a positive mode using the selected reaction monitoring (SRM) mode in the TSQ Quantiva (Thermo Scientific) mass spectrometer. The first and third quadrupoles were set up with a resolution of 0.7 (fwhm) using a cycle time of 2 s. The precursor ions fragmentation was carried out with argon gas with a CID gas pressure of 1.5 mTorr using normalized collision energy for each peptide in a range of 10−30. Regarding the ion source parameters, the spray voltage and the ion transfer tube temperature used were 2.6 kV and 280 °C, respectively, and the sweep gas was set up as 0 (Arb). The data analysis of SRM results was performed with Skyline v. 4.2 software using a public NIST library of peptide ion fragmentation spectra from Peptide Atlas (Ion Trap: Human. SpectraST format with short peptides (<7AA) excluded. File Name: NIST_human_IT_2012−05−30_7AA.splib.zip). For data normalization, we use as the global standard the heavy peptide sequence AVLDLFEETSNIGSK. For quantification analysis, we consider at least three transitions per peptides, two peptides per protein family, considering at least a dotp of 0.7. For proteins with more than one monitored peptide, the sum of normalized areas of all peptides was used for the statistical analyses. The Statistix 8.0 software was used for the calculation of the significant variations in protein abundance applying a completely randomized ANOVA test

DOI: 10.1021/acs.jproteome.9b00398
J. Proteome Res. XXXX, XXX, XXX−XXX

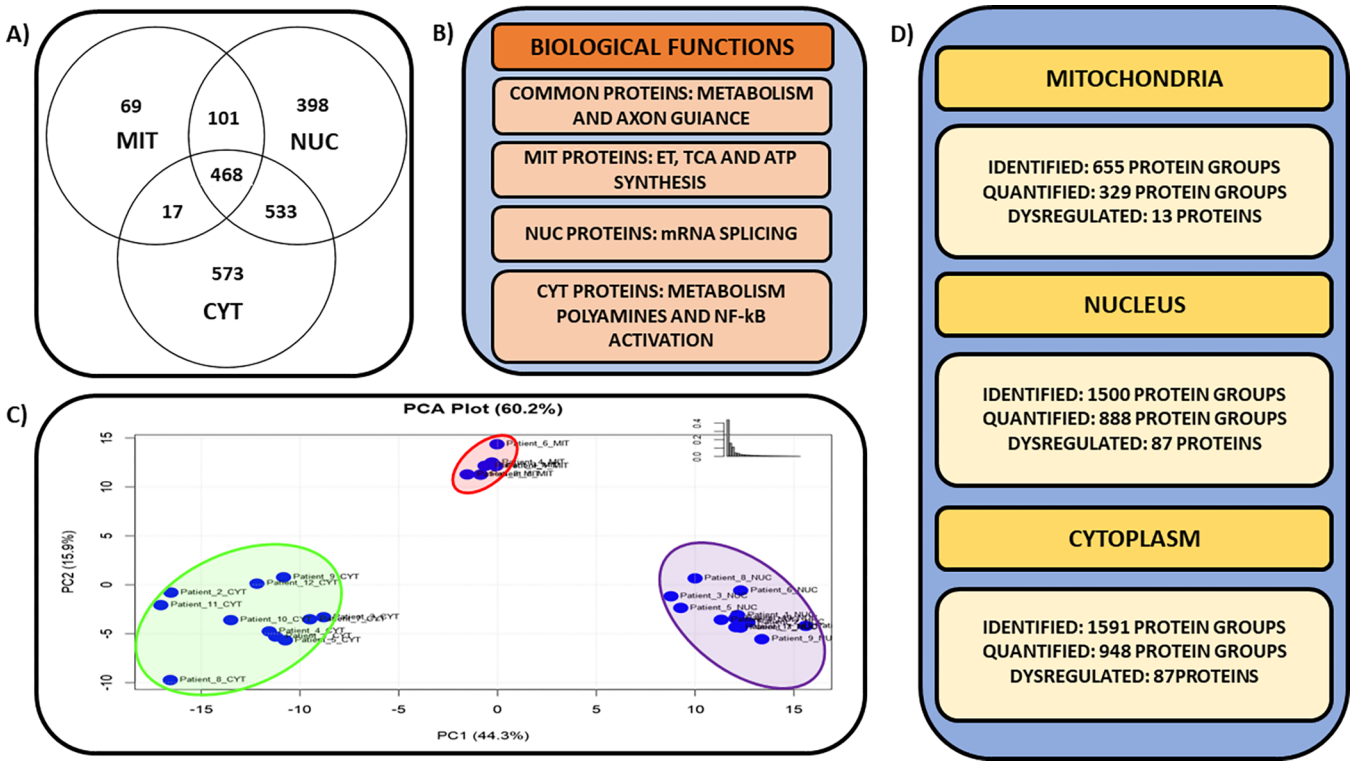

Figure 1. (A) Venn diagram of proteins identified among all cellular fractions. (B) Biological functions of the proteins identified exclusively in each subcellular fraction. (C) Principal component analysis of the patient proteome data from different fractions. (D) Total number of proteins identified, quantified, and dysregulated in each subcellular fraction.

followed by Tukey HSD all-pairwise comparisons considering a p-value <0.05.

3. RESULTS AND DISCUSSION

3.1. Proteins Identified by Mass Spectrometry

In the mass spectrometry analyses, we identified 655 protein groups from the MIT fraction, 1500 proteins groups in NUC, and 1591 protein groups in CYT (Table S-2), getting the identification of 2159 protein groups among all fractions (Figure 1). The Venn diagram reveals that the proteins identified in all fractions (17.8%) are mainly related to metabolism and axon guiance. A total of 9 % of the proteins were identified only in MIT, and they are involved in electron transport, the citric acid cycle, and ATP synthesis. The percentage of proteins found only in NUC and CYT represents 26.3% and 36%, respectively. In NUC, the biological function of these proteins is related to mRNA splicing; on the other hand, in CYT fraction proteins are involved in polyamines metabolism and NF-κB activation (Figure 1B; Table S-3). In Figure 1C, the PCA shows three well-defined different subpopulations corresponding to the patient data distribution for each fraction.

After data normalization, we applied the Grubbs test with a minimum of three peptides and p-value <0.05 per protein, in order to obtain the highest quality data for protein quantification. iTRAQ labeling robustly quantified a total of 1279 proteins, in which 329 for MIT fraction, 888 for NUC, and 948 for CYT (Figure 1D; Table S-4).

3.2. Dysregulated Proteins and Their Functional Analysis

For the selection of dysregulated proteins, in addition to the use of rigorous statistical criteria, we also consider the same quantitative behavior for up- and down-regulated proteins in at least 50% of patients. These criteria drastically reduce the number of proteins considered as dysregulated to a total of 166 in all fractions (Figure 1D; Table S-5). We performed the SRM analyses to monitor the endogenous peptides of key proteins previously quantified by iTRAQ such as γCaMKII, GS, and MAPK2 as another method to confirm the quantification of these proteins. Additionally, the label-free SRM quantification was able to monitor peptides of important proteins such as C3 and NF-kB family, who participate in key biological pathways previously quantified by the iTRAQ strategy (Table S-6).

3.2.1. Mitochondrial Fraction. Mitochondrial dysfunction and structural changes have been widely reported in schizophrenia patients.[26−28] According to a recent review[29] in post-mortem brain tissue, mitochondrial abnormalities in these patients vary according to the brain area, cell type, and also to treatment response. Thirteen proteins were found dysregulated in MIT fraction (Table S-5). We detected two proteins down-regulated, such as CLTC and PPIase A (Table S-5), related to endocytosis and protein folding, respectively. Additionally, we found 11 up-regulated proteins, mainly involved in the biological processes, such as the citric acid cycle and respiratory electron transport, mitochondrial membrane organization, and cristae formation (Table 1; Table S-7).

In our study, we found up-regulated proteins involved in mitochondrial membrane organization such as voltage-dependent anion-selective channel protein 1 (VDAC1) previously reported as dysregulated in schizophrenia patients.[27] VDAC1 overexpression mediated the mitochondrial apoptosis and its oligomerization seems to be important for the release of the pro-apoptotic proteins from the mitochondrial intermembrane space to the cytosol.[30] We also found increased the Protein

DOI: 10.1021/acs.jproteome.9b00398
J. Proteome Res. XXXX, XXX, XXX−XXX

Table 1. Proteins of the Main Dysregulated Pathways in Each Subcellular Fraction

protein ID	description	subcellular fraction	regulation	biological function	subcellular localization (Uniprot)
NX_P22695-1	cytochrome *b*-c1 complex	mitocondrial	up	aerobic respiration	mitochondrion inner membrane
NX_P50213-1	isocitrate dehydrogenase	mitocondrial	up	carbohydrate metabolic process	mitochondrion
NX_P21796-1	voltage-dependent anion-selective channel	mitocondrial	up	anion transport	mitochondrion outer membrane
NX_P09622-1	dihydrolipoyl dehydrogenase	mitocondrial	up	2-oxoglutarate metabolic process	mitochondrion matrix, nucleus
NX_P07305-1	histone H1.0 isoform	nuclear	up	apoptotic DNA fragmentation	nucleus
NX_P09429-1	high mobility group protein	nuclear	up	inflammatory response	nucleus
NX_O60313-2	dynamin-like 120 kDa protein	nuclear	up	apoptotic process	mitochondrion membrane
NX_Q15149-1	plectin isoform iso 1	nuclear	up	hemidesmosome assembly	cytoplasm
NX_P20700-1	lamin-B1	nuclear	up	interleukin-12-mediated signaling pathway	nucleus inner membrane
NX_P31946-2	14-3-3 protein beta/alpha	nuclear	up	MAPK cascade	nucleus, cytosol, mitochondrion
NX_P27348-1	14-3-3 protein theta	nuclear	up	negative regulation of transcription	nucleus, cytosol, mitochondrion
NX_P63104-1	14-3-3 protein zeta/delta	nuclear	up	apoptotic signaling pathway	nucleus, cytosol, mitochondrion
NX_Q99436-1	proteasome subunit beta type-7	cytoplasmic	down	ubiquitin-dependent protein catabolic process	cytoplasm, cell membrane
NX_P17677-1	neuromodulin	cytoplasmic	down	axon choice point recognition	cytoplasm, nucleus
NX_O43242-1	26S proteasome non-ATPase regulatory	cytoplasmic	down	ubiquitin-dependent protein catabolic process	cytoplasm, nucleus
NX_P62266-1	40S ribosomal protein S23	cytoplasmic	down	cytoplasmic translation	cytoplasm, nucleus
NX_P62847-4	40S ribosomal protein S24	cytoplasmic	down	translational initiation	cytoplasm, nucleus
NX_P35080-1	profilin-2	cytoplasmic	down	actin cytoskeleton organization	cytoplasm
NX_P04156-1	major prion protein	cytoplasmic	down	activation of protein kinase activity	cell membrane, Golgi apparatus
NX_Q01518-1	adenylyl cyclase-associated protein	cytoplasmic	down	actin polymerization or depolymerization	cell membrane
NX_Q9Y490-1	talin-1	cytoplasmic	down	ire1-mediated unfolded protein response	cytoplasm
NX_P25786-2	proteasome subunit alpha type-1	cytoplasmic	down	ubiquitin-dependent protein catabolic process	cytoplasm, nucleus
NX_P39019-1	40S ribosomal protein S19	cytoplasmic	down	translational initiation	cytoplasm, nucleus

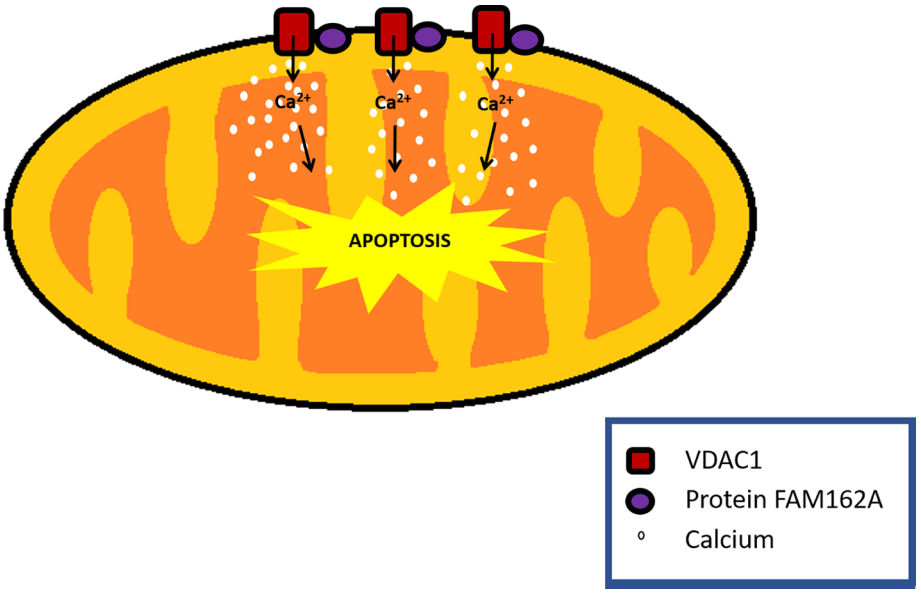

Figure 2. Representation of the main proteins involved in apoptosis from the MIT fraction. During the apoptotic process, proteins as VDAC1 and Protein FAM162A interact, leading the increase of mitochondrial Ca^{2+} uptake, triggering the apoptosis with the release of cytochrome c release. In response to the apoptotic signals, IF1 and mitochondrial cristae proteins such as Mic19 and Mic25 are overexpressed to preserve the crista architecture. Voltage-dependent anion-selective channel protein 1 (VDAC1), ATPase inhibitor (IF1).

FAM162A, who interacts with VDAC1 inducing the permeabilization of the mitochondrial transition pore, triggering the apoptosis with the release of cytochrome c and the activation of caspases.[31−33] Another indication of the

DOI: 10.1021/acs.jproteome.9b00398
J. Proteome Res. XXXX, XXX, XXX−XXX

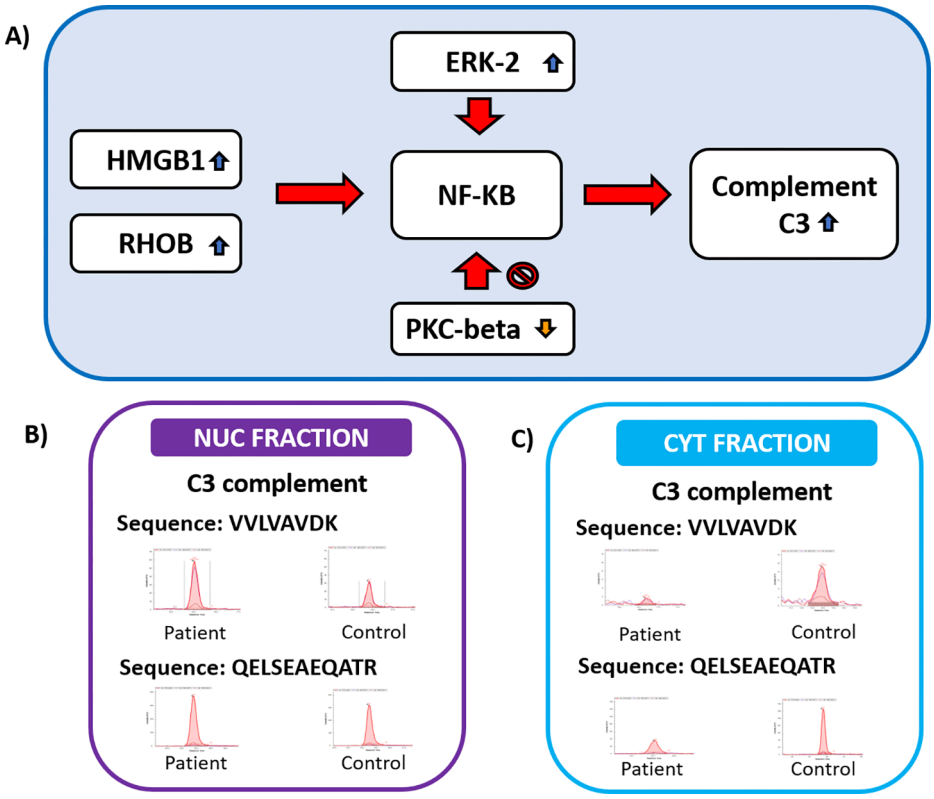

Figure 3. (A) NF-kB signaling pathway. The increase of RhoB, HMGB1, and ERK-2 together with the glutamate activate the NF-kB signaling pathway and the decrease of protein kinase C beta is involved in its regulation. NF-kB signaling pathway activation can promote the astrocytic production of complement C3. (B) Quantification of complement C3 in the NUC fraction. (C) Quantification of complement C3 in the CYT fraction. NF-kB, Nuclear Factor kappa B; RhoB, Ras Homologue Family Member B; HMGB1, High Mobility Group Box 1; ERK-2, Mitogen-activated protein kinase 1.

imbalance in apoptosis is the increase in proteins such as Complex III and NipSnap1. Under oxidative stress conditions, Complex III can trigger the intrinsic pathway of apoptosis,[34] and NipSnap1 involved in Ca^{2+} imbalance[35] can trigger the mitophagy signals.[36] These results agree with those previously reported in a study made by our group, where we analyze the synaptosome fraction of schizophrenic patients from the same brain area,[16] and we observed the deregulation of calcium metabolism pathway concomitantly with the activation of an apoptotic process (Figure 2).

When an apoptotic signal is activated, the balance between pro- and antiapoptotic stimulus determines the cell death. One of the most noticeable alterations in the apoptotic processes is the structural changes of mitochondria, and it has been suggested that mitochondrial cristae remodeling can impact Cyt c release and mitochondrial storage.[37] In response to the apoptotic signals, we found increased in schizophrenia patients the ATPase inhibitor (IF1) and mitochondrial cristae proteins such as Mic19 and Mic25. IF1 overexpression has the capacity to limit the cell death avoiding the ATP depletion from the mitochondrial matrix induced by the reverse pumping of F1Fo-ATP synthase during reduced membrane potential conditions.[38] IF1 also controls the mitochondrial cristae structure[39] and together with Mic19 and its paralog Mic25 contribute to the maintenance of the mitochondrial crista architecture and membrane organization.[40−42]

3.3. Crude Nuclear Fraction

In the NUC fraction we found 87 proteins with significant variation in their relative abundance (Table S-5). Three less abundant proteins, APP, S100A1, PRKCB, are related to Ca^{2+} signal transduction and apoptosis. On the other hand, 84 proteins increased the abundance in this subcellular fraction, and many of these are involved in apoptosis and chemical synapses transmission (Table 1; Table S-7).

3.3.1. Proteins Located in the Cell Nucleus. *3.3.1.1. Apoptosis and Chemical Synapses Transmission.* The biological function related to one of the main dysregulated protein groups is involved in the activation of apoptosis and the localization of FOXO transcription factors (Table S-7). Among these proteins, we can highlight the 14-3-3 protein family, which is involved in the regulation of various cellular events such as the apoptosis, interacting with apoptotic proteins such as BAX, BAD, and caspases,[43,44] autophagy,[45] and the MAPK activity signaling pathway.[46,47] Another function associated with the 14-3-3 protein family is the regulation of the FOXO transcription factor through phosphorylation,[48] inducing the cytoplasmic translocation of FOXO inhibiting its binding to DNA.[48,49] As a consequence, the cytoplasmic FOXO is not available to regulate the transcription of various genes like those belonging to the NF-kB signaling pathway.[50] The deficit in FOXO function leads to an increase in the in vivo activity of NF-kB.[51,52]

In parallel, we were able to detect the increase of several nuclear proteins related to NF-kB activation such as (1) RhoB[53] which can also elevate the caspase 3 in the corticohippocampal neurons,[54] (2) HMGB1, involved in the excitoneurotoxicity mediated by NF-kB[55] is released from neurons to astrocytes activating the nuclear factor-kB;[56,57] it is

DOI: 10.1021/acs.jproteome.9b00398
J. Proteome Res. XXXX, XXX, XXX−XXX

important to mention that HMGB1 activates NF-kB pathway via the ERK-dependent mechanism,[58] and in this sense, we have detected by SRM the protein ERK-2 which is increased in the NUC fraction (Table S-6), indirect evidence of ERK activation.[59] Also, we found down-regulation of the nuclear Protein kinase C beta involved in NF-kB regulation[60,61] (Figure 3A). A microarray profiled from the superior temporal gyrus of patients with schizophrenia suggest that NF-kB signaling is down-regulated in this brain area,[62] but a recent study of Volk and colleagues[63] extensively map the expression of genes related to NF-kB signaling through the canonical and noncanonical pathways in the prefrontal cortex of schizophrenia patients, concluding that both pathways are increased and they are not affected by the antipsychotic treatment.

On the other hand, we found deregulated proteins that stand out for participating in the chemical synapses transmission, represented principally with the increase of proteins as calcium/calmodulin-dependent protein kinase type II gamma (γCaMKII). γCaMKII is a shuttle protein that binds Ca^{2+}/CaM. After the cytosolic increase of Ca^{2+}, γCaMKII translocates CaM from the cytoplasm to the nucleus.[64] This protein was reported previously up-regulated (together with CaM) in a nuclear fraction from the corpus callosum and anterior temporal lobe of schizophrenia patients;[15] also it was shown that γCaMKII has an abnormal regulation in the prefrontal cortex by the miR-219 in the dizocilpine murine model.[65] γCaMKII unique peptides were mapped and quantified using the SRM technique in the NUC and CYT fractions (where previously it could not be identified) demonstrating that γCaMKII apparently is mainly located in NUC since it was found increased in that fraction and no significant change in CYT. However, how can the nuclear γCaMKII be increased in our results if the nuclear CaM have the tendency to remain decreased? (Table S-5). Previously, studies demonstrated that γCaMKII needs to be phosphorylated in Thr287 for effective CaM nuclear delivery[66,67] and for this process, it was shown that βCaMKII kinase function is responsible for pThr287.[66] In accordance with these observations, we found βCaMKII down-regulated in the CYT fraction. Ma and colleagues (2014) elegantly demonstrated that without βCaMKII phosphorylation at T287, the nuclear translocation of the γCaMKII is not affected but nuclear delivery of CaM and CREB activation is impaired[66] (Figure 4). Imbalance in CREB activation is detrimental to synaptic plasticity.[68]

The crude nuclear fraction obtained during the sample processing, in addition to enriching nuclear proteins, brings common contaminants such as mitochondria (especially those located in the perinuclear region), sheets of the plasma membrane, and also, possibly, minor contaminants such as lysosomes, peroxisomes, Golgi membranes, and various membrane vesicles.[69] The methodology implemented restricts the interpretation of the biological function of proteins that can share different subcellular locations besides the nucleus, in this data set, we detect as the main contaminants of the NUC fraction, proteins whose more frequent subcellular location has been reported in mitochondrion and cellular membrane; nevertheless, some of these proteins are interesting to mention due to their biological importance.

3.3.2. Mitochondrial Proteins Present in the Crude Nuclear Fraction. We quantified proteins in the crude nuclear fraction whose subcellular location has been reported only in the mitochondrion and for which in the MIT fraction we have not identified or observed any significant variation in the relative abundance compared to the control group. What could, then, explain that these proteins do not significantly change their abundance in the MIT fraction and, at the same time, are dysregulated in this crude nuclear fraction? One possible answer is that these proteins have a nuclear function not yet described or, the most plausible explanation is that these proteins could reflect the activity of the perinuclear mitochondria, due to the technical limitations mentioned above for this type of enrichment for nuclear proteins. Since a long time ago, the heterogeneity of mitochondria in a single cell has been reported.[70] In the same cell, the mitochondria can be morphologically heterogeneous in terms of ultrastructure, cristae density, and shape, having different respiratory status and functional properties as divergences in Ca^{2+} and reactive oxygen species (ROS) levels, protein composition, mitochondrial membrane potential, different response to apoptotic and mitophagy signals, and also different fission and fusion dynamics.[70−74]

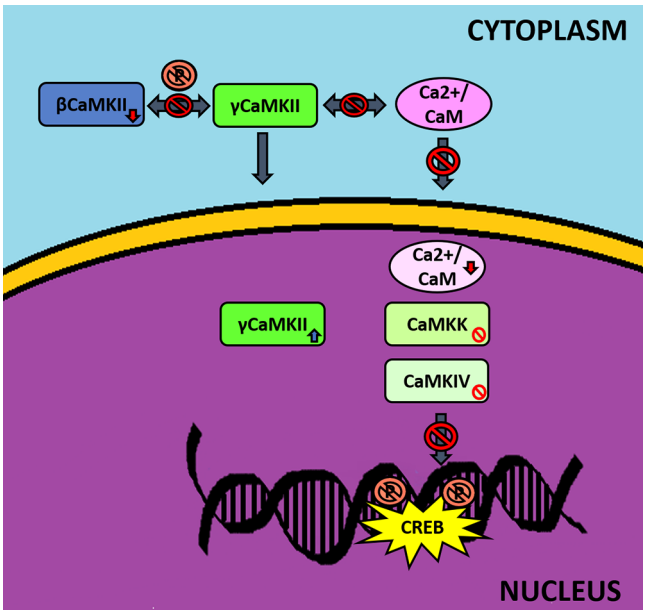

Figure 4. CREB imbalance hypothesis by γCaMKII. Cytoplasmatic βCaMKII quantified as down-regulated in the CYT fraction was reported as a key kinase that phosphorylates γCaMKII. It is represented how the low availability of βCaMKII could affect γCaMKII phosphorylation which would impact γCaMKII/Ca^{2+}/CaM interaction. The inappropriate interaction between γCaMKII with Ca^{2+}/CaM can lead to an inefficient nuclear shuttle of Ca^{2+}/CaM by γCaMKII. Inappropriated γCaMKII shuttles can impact CREB activation by other Ca^{2+}/CaM dependent kinases such as CaMKK, CaMKIV, and αCaMKII. CREB, Ca^{2+}/cAMP response element-binding protein; βCaMKII, calcium/calmodulin-dependent protein kinase beta; γCaMKII, calcium/calmodulin-dependent protein kinase gamma; Ca^{2+}/CaM, calcium/calmodulin.

Among these mitochondrial proteins, those belonging to the electron transport chain are dysregulated. We found several subunits of the NADH dehydrogenase (Complex I) as up-regulated in our data set. Complex I subunits were previously reported down-regulated in post-mortem brain tissues from different brain areas in schizophrenia patients,[13,75,76] and it was demonstrated that antipsychotic treatment and early onset of illness have a strong correlation with Complex I decline.[75] On the other hand, the mRNA expression of certain Complex I subunits was significantly higher in blood samples of the

DOI: 10.1021/acs.jproteome.9b00398
J. Proteome Res. XXXX, XXX, XXX−XXX

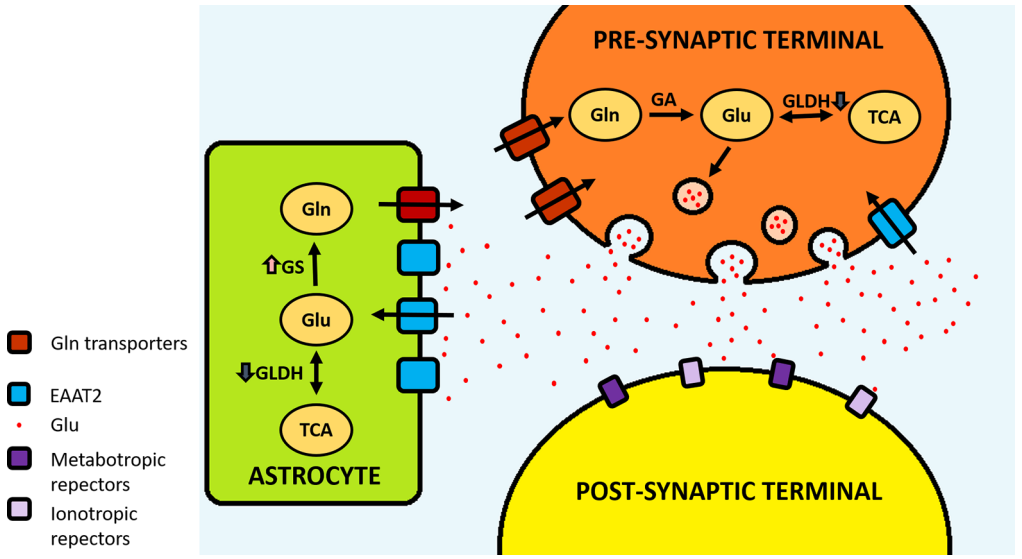

Figure 5. Dysregulation in glutamate metabolism. In astrocytes, the glutamate is taken up from the synaptic cleft by the excitatory amino acid transporters and converted to glutamine by glutamine synthetase (GS). In the presynaptic terminal, the glutamine is transported and it is converted back into glutamate by glutaminase (GA). The deviation of the metabolism toward the preferential production of glutamine is also favored by the decrease of GLDH in astrocytes and neurons. Gln, glutamine; Glu, glutamate; EAAT2, excitatory amino acid transporters 2; GLDH, glutamate dehydrogenase; TCA, tricarboxylic acid cycle.

schizophrenia group, having a positive correlation with the first-episode schizophrenia subgroup.[77] It still did not fully elucidate the biological meaning about the discrepancy in the abundance of the different complex I subunits, nevertheless, impairments in mitochondrial metabolism have been associated with cognitive and behavioral abnormalities during the clinical course of schizophrenia.[77]

Another set of key proteins that we detect in this fraction were those related to the glutamate metabolism such as glutamine synthetase (GS) increased in the NUC fraction and glutamate dehydrogenase (GLDH) found as decreased in the CYT fraction (Figure 5). Almost all of them are located in the astrocytes, where the glutamate is taken up from the synaptic cleft and converted to glutamine by GS or in α-ketoglutarate by GLDH.[78] On the other hand, once the glutamine is produced in the astrocytes, it is transported to the neurons where it is converted back into glutamate by the glutaminase GA,[79] and we observe a tendency of the increase of this protein in our patients (Table S-5).

Over the years, the deregulation of glutamate has been formulated as one of the main hypotheses in the pathophysiology of schizophrenia in patients. High levels of glutamate plus glutamine have been reported in unmedicated patients when they are compared with healthy subjects.[80] GS transcripts have been reported as up-regulated in schizophrenia thalamus suggesting the enhanced glutamatergic neurotransmission.[81] Moreover, GS was found decreased in the prefrontal cortex and increased in the anterior cingulate and cerebellar cortex whereas no significant differences were observed in the posterior cingulate cortex.[82] Despite this, a study points out that there are no significant differences between the GS activity in the prefrontal cortex of schizophrenia patients and controls.[83] In this case, we monitor GS by SRM confirming that it is increased in our patients (Table-S6) suggesting that glutamine production can be dysregulated in these patients. On the other hand, the level of platelet GLDH before antipsychotic treatment has been reported as significantly lower[84] and higher in post-mortem brain tissues from the prefrontal cortex of chronic schizophrenia patients.[83] Nevertheless, in a study performed by Lander and colleges,[85] the gene expression profile of Glud-1 was found down-regulated in the CA1 region of schizophrenia patients, proving that Glud-1 deficient mouse had an elevated excitatory/inhibitory balance in CA1 region with similar behavioral abnormalities to the schizophrenia symptoms.

3.3.3. Membrane Proteins Present in the Crude Nuclear Fraction. The first cluster of proteins dysregulated that we would like to highlight are those related to glutamate pathways, such as excitatory amino acid transporter 2 (EAAT2), whose main function is the regulation of total glutamate uptake (Figure 5). EAAT2 is localized in the plasma membrane of astrocytes but also in other cells as oligodendrocytes, microglia; and recently EAAT2 was also identified in neurons.[86] EAAT2 is the main transporter, responsible for about 90% of the glutamate clearance in the synaptic cleft.[87]

The different amounts of transcript and protein levels of EAATs in diverse brain areas of schizophrenia patients are reported. Any variation in the amount of EAAT2 transcript or protein level in the dorsolateral prefrontal cortex of schizophrenia patients was not detected.[88] However, in another study from the prefrontal cortex of medication-free schizophrenia patients, the mRNA levels of EAAT2 was increased compared to the controls;[89] in fact, the data reveals that in the thalamus, the in excitatory neurons had a compensatory increment of the EAAT2 mRNA expression, suggesting an impairment in the clearance of glutamate capacity by astrocytes and decoupled glutamate metabolism in the tripartite synapse.[90]

The second group of proteins that we would like to mention is involved in the complement system pathway. First, we quantified as up-regulated the CD59 glycoprotein, an important cell membrane whose main function is the inhibition of C9 complement molecule to prevent the pore membrane attack complex (MAC).[91] In Alzheimer disease, it was observed that CD59 activation is not efficient to suppress the complement pathway.[92] Recently, it was described the

DOI: 10.1021/acs.jproteome.9b00398
J. Proteome Res. XXXX, XXX, XXX−XXX

activation of the complement pathway through the NF-kB signaling. Astrocytes are one of the main sources of NF-kB, which promote the production of complement C3, C3R neuronal receptors stimulation, calcium imbalance, and morphological change in dendrites.[93] Based on this information and in the evidence of NF-kB dysregulation in our data, we decided to implement a targeted approach to quantify the complement C3 and members of the NF-kB family using SRM (Table S-6). We observed that C3 is increased in schizophrenia patients compared to the control only in the NUC fraction, which probably indicates, due to the technical limitations related to the enrichment of this fraction mentioned above, the location of C3 in the plasma membrane and the activation of the complement pathway (Figure 3B,C). The NF-kB family members such as NF-kB1 and NF-kB2 were also increased in the NUC fraction (Table S-6), suggesting an important role of this pathway as a possible mechanism for C3 activation. Complement proteins are required for the central nervous system to carry out the elimination of inappropriate synapses.[94] The expression of C3 fragments on the cell surface also allows the recognition of this signal by microglia CR3 receptors promoting the engulfment of synaptic elements.[95] This process could participate in the active elimination of long-term depression synapses when apoptotic mechanism as caspase-3 cascade is activated in dendrites without causing cell death.[96,94]

Over the years, the complement system has been indicated as an important element in the schizophrenia pathogenesis. Recently, one of the most extensive genetic studies links the human major histocompatibility complex as one of the most significant loci related to schizophrenia.[9] In 2016, Sekar and colleagues[97] have reported elevated expression of the C4A transcript in schizophrenia patients, reinforcing the theory that C4 leads the C3 activation and the synapsis elimination.

3.4. Cytoplasmatic Fraction

In the CYT fraction, we quantified 87 dysregulated proteins (Table S-5). This fraction stands out because most of the proteins, that fulfilled our selection criteria, are not only down-regulated but counter-regulated in relation to the other fractions, that is, the same protein is mostly up-regulated in the NUC or/and in the MIT fraction. The biological functions associated with these proteins are the axon guidance process which also includes the dysregulation of the proteasome proteins and ribosomal proteins (Table 1; Table S-7).

One of the main proteins involved in axon guidance, neuronal outgrowth, and synaptic plasticity is neuromodulin (GAP-43), which decreased in the schizophrenia cohort. GAP-43 down-regulation inhibits the initiation of axonal regrowth after axotomy.[98] In schizophrenia, subjects observed a significant reduction of GAP-43 in the dentate gyrus.[99] Moreover, the astrocytic GAP43 knockdown induces the overexpression of EAAT2 that causes the excessive extracellular glutamate uptake activating the astrocyte-induced neurotoxicity and microglial activation.[100]

Ribosomal proteins is another important cluster that also participates in the axonal growth with the local mRNA translation.[101] We found the ribosomal proteins (RP) decreased principally, from the 60S and 40S ribosomal subunits (RS), responsible for catalyzing, during the protein synthesis process, the peptide bond formation, and for binding, decoding, and pairing the mRNAs codons and aminoacylated tRNAs, respectively.[102] New protein synthesis is essential for axon guidance, structural remodeling, and functional change behind the long-term potentiation and depression to establish new synaptic connections and/or strength the pre-existing synaptic communication, the molecular basis for memory formation and maintenance.[103] An integrated study of proteomics and transcriptomic analysis using the human olfactory neurosphere-derived from a schizophrenia patient detect a significant reduction in 17 ribosomal proteins with a lower global protein synthesis rates compared with the control, and also a dysregulation was noticed in the upstream signaling pathways that control the protein synthesis such as the eIF2 and mTOR signaling.[104]

Nevertheless, in this study, our data set reveals something else about the ribosomal protein cluster. When we look at the quantification in the other fractions, specifically in the NUC fraction, two of that RP are up-regulated in NUC. For years, the role of the extraribosomal function of RS in different physiological and pathological processes, especially during ribosomal stress, development, immune response, and tumorigenesis has been investigated.[105] The main functions of the dysregulated RP with extraribosomal function are described in Table 2.

Table 2. Extra-Ribosomal Functions of Ribosomal Subunits[a]

ribosomal protein	CYT fraction	NUC fraction	extra-ribosomal function	ref
S19	↓	↑	inhibition of Mif, ERK and NF-kB	106,107
L23	n.q.	↑	p53 activation. regulation of Miz1 function.	109,110,128
S23	↓	n.q	Sre1 activity modulation (yeast)	129
L28	=	↑	extraribosomalfunctions unknown	

[a]n.q, not quantified. =, nonsignificant quantitative changes.

Among all quantified RP, we can highlight S19 and L23. S19 inhibits the Macrophage migration inhibitory factor (MIF) and prevents its transcription and protein expression.[106,107] MIF-knockout is characterized by the increase in caspase 3 activity and down-regulation of MIF, under hypoxia conditions, incrementing the neuronal loss through the NF-kB signaling.[108] On the other hand, L23 inhibits the transactivation of MIZ1, a protein responsible for the activation of genes that control cell arrest cycle in carcinoma cell lines.[109,110] Furthermore, in our NUC proteins set, we found to increase the Far upstream element-binding protein 1, a regulator that induces the overexpression of MYC,[111,112] a key protein with opposite biological functions, depends on the cellular context, cell proliferation, and apoptosis.[113] Specifically, in neurons, MYC overexpression promotes the activation of the cell cycle leading to neuronal cell death[114,115] and participates in the apoptotic response mediated by NF-kB signaling in response to neuronal excitotoxicity.[116] Among all its functions, MYC also regulates the expression of the target gene of L23[110] and can inhibit MIZ1 as well as L23.[117] In myelodysplastic syndrome, the RPL23/Miz-1/c-Myc circuit provides a regulatory feedback to lead to apoptotic resistance;[118] nevertheless, it was reported that in fibroblast models, MIZ1 inactivation is essential for MYC apoptotic function not for cell cycle progression and transformation.[119] However, in the context of nervous system cells (NSC), it has been described as different functions for MIZ1 such as the regulation of genes

DOI: 10.1021/acs.jproteome.9b00398
J. Proteome Res. XXXX, XXX, XXX−XXX

responsible for vesicular transport and autophagy.[120] Until the moment, the function of L23-MIZ1 in the cells of the nervous system has not been described, but it is possible that L23 could exert a regulation of the MIZ1 function on the transcription of this type of gene in the NSC. Although, despite the lack of evidence in this sense, it is curious that in our data, we observed the decreased of proteins such as the TBC1 domain family member 24 which have related functions to those observed by Wolf and collaborators,[120] but the biological functions of L23-MIZ1-Myc remain to be elucidated in schizophrenia physiopathology.

Finally, proteins belonging to the ubiquitin-proteasome system (UPS) were found dysregulated. UPS is the main system for protein degradation but acts in receptor recycling, vesicle trafficking, vacuolar degradation,[121] and axon development.[122] The decrease of the UPS system in the superior temporal gyrus and dentate granule neurons of individuals with schizophrenia results in impairment of AMPAR homeostasis, an abnormal structure in the dendritic spine and accumulation of aberrant proteins in the endoplasmic reticulum (ER).[123,124] An inefficient UPS can make the neurons more vulnerable to reactive oxygen species contributing to the mitochondrial impairments reported in schizophrenia.[124]

4. CONCLUSION

OFC is a brain area that plays a key role in sensory integration and feedback processing. Changes in OFC volume gray matter is associated with the severity of negative as well as cognitive deficits in schizophrenia. In a previous study of this same brain area, we perform the proteomic characterization of the synaptosome fraction, finding as one of the main dysregulated routes the calcium signaling pathway together with proteins involved in ER stress and activation of the apoptosis process.[16]

Following our previous results,[16] one of our first conclusions is that activation of apoptosis is important in the physiopathology of schizophrenia, at least in the OFC. This is reflected in the increase of pro-apoptotic proteins in MIT as VDAC1, Protein FAM162A, and Complex III. Second, the decreased in the abundance of cytoplasmatic βCaMKII may impact the nuclear function of γCaMKII[66] with a negative impact in a Ca^{2+}/CaM shuttle and CREB activation impairments associated with cognitive disability in schizophrenia patients.

The dysregulation of glutamate metabolism apparently happens in the regulation of its synthesis and clearance from the synaptic cleft, simultaneously with impairment of the cytoplasmatic membrane traffic, which impact EAATs regulation. Evidence indicates that glutamate dysregulation can lead to synaptic damage and neuron death, with a marker of behavioral and cognitive dysfunction.[125] Also, glutamate can activate the NF-kB pathway.[126] One of the most important findings of this study is the overexpression of proteins intimately related to the NF-kB signaling pathway. In the NUC fraction, we found the activation of the 14-3-3 protein family, RhoB, HMGB1; in the same way, we also found in the NUC and CYT fractions proteins involved in the regulation of NF-kB signaling as Protein kinase beta and L23, respectively, as well as proteins that can induce neuronal loss through the NF-kB pathway, for instance, S19 by means of MIF down-regulation.

Finally, the abnormality in the cytoarchitecture of schizophrenia patients' brains has been widely reported, and this evidence indicates that the loss of volume in the OFC is not a consequence of the antipsychotic drug treatment.[127] As we mentioned earlier, in astrocytes the NF-kB signaling pathway activation can promote the astrocytic production of C3, stimulating the C3R neuronal receptors which entail a calcium imbalance and changes in neural morphology.[93] Our data reveal the increase of the complement system C3 in the OFC. The expression of C3 can promote and excessive synaptic pruning by microglia engulfment constituting one of the possible main mechanisms of gray matter loss in schizophrenia patients. Based on our data analysis, we suggest the activation of NF-kB as a possible pathway that links the deregulation of glutamate, calcium, apoptosis, and the activation of the immune system in schizophrenia patients.

■ ASSOCIATED CONTENT

Supporting Information

The Supporting Information is available free of charge on the ACS Publications website at DOI: 10.1021/acs.jproteome.9b00398.

Supporting Table S-1, clinical information on patients and controls (XLSX)

Supporting Table S-2, group of proteins and peptides identified by iTRAQ in each enrichment of subcellular fraction (XLSX)

Supporting Table S-3, reactome pathway analysis of the proteome from each enriched subcellular fraction (XLSX)

Supporting Table S-4, group of proteins quantified after InfernoRND normalization (XLSX)

Supporting Table S-5, dysregulated proteins quantified by iTRAQ in each enriched subcellular fraction (XLSX)

Supporting Table S-6, selected reaction monitoring analysis of proteins as γCaMKII, MAPK2, GS, C3, and NF-kB family (XLSX)

Supporting Table S-7, biological analysis of dysregulated proteins quantified by iTRAQ of each enriched subcellular fraction (XLSX)

■ AUTHOR INFORMATION

Corresponding Authors

*E-mail: gilberto@iq.ufrj.br.

*E-mail: fabiocsn@iq.ufrj.br.

ORCID

Gilberto B. Domont: 0000-0002-1329-6483

Fabio C. S. Nogueira: 0000-0001-5507-7142

Notes

The authors declare no competing financial interest.

All MS data are available in the ProteomeXchange Repository under the identifier PXD015356 and PXD014350.

The authors recognize that the protein-level FDR is an estimate based on several imperfect assumptions and present the FDR with appropriate precision and acknowledge that not all proteins surviving the threshold are "confidently identified".

■ ACKNOWLEDGMENTS

D.M.-d.-S. is supported by the São Paulo Research Foundation (FAPESP), Grants 2017/25588-1 and 2019/00098-7 and the Brazilian National Council for Scientific and Technological Development (CNPq) Grant 302453/2017-2. E.V. thanks CNPq for her Ph.D. scholarship. F.C.S.N. acknowledges Grant

DOI: 10.1021/acs.jproteome.9b00398
J. Proteome Res. XXXX, XXX, XXX−XXX

E-26/202.650/2018 from the Rio de Janeiro State Foundation for Science Support (FAPERJ), and G.B.D. acknowledges CNPq Grant 306316/2015-3.

REFERENCES

(1) Patel, K. R.; Cherian, J.; Gohil, K.; Atkinson, D. Schizophrenia: Overview and Treatment Options. *P T* **2014**, *39* (9), 638−645.

(2) Stepnicki, P.; Kondej, M.; Kaczor, A. A. Current Concepts and Treatments of Schizophrenia. *Molecules* **2018**, *23* (8), 2087.

(3) Möller, H.-J. The Relevance of Negative Symptoms in Schizophrenia and How to Treat Them with Psychopharmaceuticals? *Psychiatr. Danub.* **2016**, *28* (4), 435−440.

(4) Gao, W.-J.; Wang, H.-X.; A, M.; Li, Y.-C. The Unique Properties of the Prefrontal Cortex and Mental Illness. In *When Things Go Wrong - Diseases and Disorders of the Human Brain*; InTech, 2012; DOI: 10.5772/35868.

(5) Jackowski, A. P.; de Araujo Filho, G. M.; de Almeida, A. G.; de Araujo, C. M.; Reis, M.; Nery, F.; Batista, I. R.; Silva, I.; Lacerda, A. L.T. The Involvement of the Orbitofrontal Cortex in Psychiatric Disorders: An Update of Neuroimaging Findings. *Rev. Bras. Psiquiatr.* **2012**, *34* (2), 207−212.

(6) Takayanagi, Y.; Takahashi, T.; Orikabe, L.; Masuda, N.; Mozue, Y.; Nakamura, K.; Kawasaki, Y.; Itokawa, M.; Sato, Y.; Yamasue, H.; et al. Volume Reduction and Altered Sulco-Gyral Pattern of the Orbitofrontal Cortex in First-Episode Schizophrenia. *Schizophr. Res.* **2010**, *121* (1−3), 55−65.

(7) Kanahara, N.; Sekine, Y.; Haraguchi, T.; Uchida, Y.; Hashimoto, K.; Shimizu, E.; Iyo, M. Orbitofrontal Cortex Abnormality and Deficit Schizophrenia. *Schizophr. Res.* **2013**, *143* (2−3), 246−252.

(8) Ohtani, T.; Bouix, S.; Hosokawa, T.; Saito, Y.; Eckbo, R.; Ballinger, T.; Rausch, A.; Melonakos, E.; Kubicki, M. Abnormalities in White Matter Connections between Orbitofrontal Cortex and Anterior Cingulate Cortex and Their Associations with Negative Symptoms in Schizophrenia: A DTI Study. *Schizophr. Res.* **2014**, *157* (1−3), 190−197.

(9) Schizophrenia Working Group of the Psychiatric Genomics Consortium. Biological Insights from 108 Schizophrenia-Associated Genetic Loci. *Nature* **2014**, *511* (7510), 421−427.

(10) Enwright, J. F.; Huo, Z.; Arion, D.; Corradi, J. P.; Tseng, G.; Lewis, D. A. Transcriptome Alterations of Prefrontal Cortical Parvalbumin Neurons in Schizophrenia. *Mol. Psychiatry* **2018**, *23* (7), 1606−1613.

(11) Arion, D.; Huo, Z.; Enwright, J. F.; Corradi, J. P.; Tseng, G.; Lewis, D. A. Transcriptome Alterations in Prefrontal Pyramidal Cells Distinguish Schizophrenia From Bipolar and Major Depressive Disorders. *Biol. Psychiatry* **2017**, *82* (8), 594−600.

(12) Sanders, A. R.; Drigalenko, E. I.; Duan, J.; Moy, W.; Freda, J.; Goring, H. H. H.; Gejman, P. V. Transcriptome Sequencing Study Implicates Immune-Related Genes Differentially Expressed in Schizophrenia: New Data and a Meta-Analysis. *Transl. Psychiatry* **2017**, *7* (4), e1093.

(13) Nascimento, J. M.; Martins-De-Souza, D. The Proteome of Schizophrenia. *npj Schizophr* **2015**, *1* (1), 14003.

(14) Shan, D.; Mount, D.; Moore, S.; Haroutunian, V.; Meador-Woodruff, J. H.; McCullumsmith, R. E. Abnormal Partitioning of Hexokinase 1 Suggests Disruption of a Glutamate Transport Protein Complex in Schizophrenia. *Schizophr. Res.* **2014**, *154* (1−3), 1−13.

(15) Saia-Cereda, V. M.; Santana, A. G.; Schmitt, A.; Falkai, P.; Martins-De-Souza, D. The Nuclear Proteome of White and Gray Matter from Schizophrenia Postmortem Brains. *Mol. Neuropsychiatry* **2017**, *3* (1), 37−52.

(16) Velásquez, E.; Nogueira, F. C. S.; Velásquez, I.; Schmitt, A.; Falkai, P.; Domont, G. B.; Martins-De-Souza, D. Synaptosomal Proteome of the Orbitofrontal Cortex from Schizophrenia Patients Using Quantitative Label-Free and ITRAQ-Based Shotgun Proteomics. *J. Proteome Res.* **2017**, *16* (12), 4481−4494.

(17) Itzhak, D. N.; Tyanova, S.; Cox, J.; Borner, G. H. H. Global, Quantitative and Dynamic Mapping of Protein Subcellular Localization. *eLife* **2016**, *5*, e16950.

(18) *DSM-IV: Diagnostic and Statistical Manual of Mental Disorder*, 4th ed.; American Psychiatric Association, 1994.

(19) Larsen, M. R.; Thingholm, T. E.; Jensen, O. N.; Roepstorff, P.; Jørgensen, T. J. D. *Mol. Cell. Proteomics* **2005**, *4*, 873−886.

(20) Polpitiya, A. D.; Qian, W. J.; Jaitly, N.; Petyuk, V. A.; Adkins, J. N.; Camp, D. G.; Anderson, G. A.; Smith, R. D. DAnTE: A Statistical Tool for Quantitative Analysis of -Omics Data. *Bioinformatics* **2008**, *24* (13), 1556−1558.

(21) The UniProt Consortium.. UniProt: The Universal Protein Knowledgebase. *Nucleic Acids Res.* **2017**, *45* (D1), D158−D169.

(22) Oliveros, J. C. *Venny 2.1*, an interactive tool for comparing lists with Venn Diagrams, http://bioinfogp.cnb.csic.es/tools/venny/index.html.

(23) Fabregat, A.; Sidiropoulos, K.; Garapati, P.; Gillespie, M.; Hausmann, K.; Haw, R.; Jassal, B.; Jupe, S.; Korninger, F.; McKay, S.; et al. The Reactome Pathway Knowledgebase. *Nucleic Acids Res.* **2016**, *44* (D1), D481−D487.

(24) Szklarczyk, D.; Franceschini, A.; Wyder, S.; Forslund, K.; Heller, D.; Huerta-Cepas, J.; Simonovic, M.; Roth, A.; Santos, A.; Tsafou, K. P.; et al. STRING V10: Protein-Protein Interaction Networks, Integrated over the Tree of Life. *Nucleic Acids Res.* **2015**, *43* (D1), D447−D452.

(25) Ogata, H.; Goto, S.; Sato, K.; Fujibuchi, W.; Bono, H.; Kanehisa, M. KEGG: Kyoto Encyclopedia of Genes and Genomes. *Nucleic Acids Res.* **1999**, *27* (1), 29−34.

(26) Iwamoto, K.; Bundo, M.; Kato, T. Altered Expression of Mitochondria-Related Genes in Postmortem Brains of Patients with Bipolar Disorder or Schizophrenia, as Revealed by Large-Scale DNA Microarray Analysis. *Hum. Mol. Genet.* **2005**, *14* (2), 241−253.

(27) English, J. A.; Pennington, K.; Dunn, M. J.; Cotter, D. R. The Neuroproteomics of Schizophrenia. *Biol. Psychiatry* **2011**, *69* (2), 163−172.

(28) Robicsek, O.; Ene, H. M.; Karry, R.; Ytzhaki, O.; Asor, E.; McPhie, D.; Cohen, B. M.; Ben-Yehuda, R.; Weiner, I.; Ben-Shachar, D. Isolated Mitochondria Transfer Improves Neuronal Differentiation of Schizophrenia-Derived Induced Pluripotent Stem Cells and Rescues Deficits in a Rat Model of the Disorder. *Schizophr. Bull.* **2018**, *44* (2), 432−442.

(29) Roberts, R. C. Postmortem Studies on Mitochondria in Schizophrenia. *Schizophr. Res.* **2017**, *187*, 17−25.

(30) Weisthal, S.; Keinan, N.; Ben-Hail, D.; Arif, T.; Shoshan-Barmatz, V. Ca2+-Mediated Regulation of VDAC1 Expression Levels Is Associated with Cell Death Induction. *Biochim. Biophys. Acta, Mol. Cell Res.* **2014**, *1843* (10), 2270−2281.

(31) Lee, M.; Kim, J.; Suk, K.; Park, J. Identification of the Hypoxia-Inducible Factor 1_-Responsive HGTD-P Gene as a Mediator in the Mitochondrial Apoptotic Pathway. *Mol. Cell. Biol.* **2004**, *24* (9), 3918−3927.

(32) Cho, Y. E.; Ko, J. H.; Kim, Y. J.; Yim, J. H.; Kim, S. M.; Park, J. H. MHGTD-P Mediates Hypoxic Neuronal Cell Death via the Release of Apoptosis-Inducing Factor. *Neurosci. Lett.* **2007**, *416* (2), 144−149.

(33) Qu, Y.; Mao, M.; Zhao, F.; Zhang, L.; Mu, D. Proapoptotic Role of Human Growth and Transformation-Dependent Protein in the Developing Rat Brain after Hypoxia-Ischemia. *Stroke* **2009**, *40* (8), 2843−2848.

(34) Dibrova, D. V.; Cherepanov, D. A.; Galperin, M. Y.; Skulachev, V. P.; Mulkidjanian, A. Y. Evolution of Cytochrome Bc Complexes: From Membrane-Anchored Dehydrogenases of Ancient Bacteria to Triggers of Apoptosis in Vertebrates. *Biochim. Biophys. Acta, Bioenerg.* **2013**, *1827* (11−12), 1407−1427.

(35) Schoeber, J. P. H.; Topala, C. N.; Lee, K. P.; Lambers, T. T.; Ricard, G.; Van Der Kemp, A. W. C. M.; Huynen, M. A.; Hoenderop, J. G. J.; Bindels, R. J. M. Identification of Nipsnap1 as a Novel Auxiliary Protein Inhibiting TRPV6 Activity. *Pfluegers Arch.* **2008**, *457* (1), 91−101.

DOI: 10.1021/acs.jproteome.9b00398
J. Proteome Res. XXXX, XXX, XXX−XXX

(36) Princely Abudu, Y.; Pankiv, S.; Mathai, B. J.; Håkon Lystad, A.; Bindesbøll, C.; Brenne, H. B.; Yoke Wui Ng, M.; Thiede, B.; Yamamoto, A.; Mutugi Nthiga, T.; et al. NIPSNAP1 and NIPSNAP2 Act as "Eat Me" Signals for Mitophagy. *Dev. Cell* **2019**, *49* (4), 509−525.
(37) Frezza, C.; Cipolat, S.; Martins de Brito, O.; Micaroni, M.; Beznoussenko, G. V.; Rudka, T.; Bartoli, D.; Polishuck, R. S.; Danial, N. N.; De Strooper, B.; et al. OPA1 Controls Apoptotic Cristae Remodeling Independently from Mitochondrial Fusion. *Cell* **2006**, *126* (1), 177−189.
(38) Campanella, M.; Parker, N.; Tan, C. H.; Hall, A. M.; Duchen, M. R. IF1: Setting the Pace of the F1Fo-ATP Synthase. *Trends Biochem. Sci.* **2009**, *34* (7), 343−350.
(39) Faccenda, D.; Nakamura, J.; Gorini, G.; Dhoot, G. K.; Piacentini, M.; Yoshida, M.; Campanella, M. Control of Mitochondrial Remodeling by the ATPase Inhibitory Factor 1 Unveils a Pro-Survival Relay via OPA1. *Cell Rep.* **2017**, *18* (8), 1869−1883.
(40) Darshi, M.; Mendiola, V. L.; Mackey, M. R.; Murphy, A. N.; Koller, A.; Perkins, G. A.; Ellisman, M. H.; Taylor, S. S. ChChd3, an Inner Mitochondrial Membrane Protein, Is Essential for Maintaining Crista Integrity and Mitochondrial Function. *J. Biol. Chem.* **2011**, *286* (4), 2918−2932.
(41) An, J.; Shi, J.; He, Q.; Lui, K.; Liu, Y.; Huang, Y.; Sheikh, M. S. CHCM1/CHCHD6, Novel Mitochondrial Protein Linked to Regulation of Mitofilin and Mitochondrial Cristae Morphology. *J. Biol. Chem.* **2012**, *287* (10), 7411−7426.
(42) Friedman, J. R; Mourier, A.; Yamada, J.; McCaffery, J M.; Nunnari, J. MICOS Coordinates with Respiratory Complexes and Lipids to Establish Mitochondrial Inner Membrane Architecture. *eLife* **2015**, *4*, e07739.
(43) Rosenquist, M. 14−3-3 Proteins in Apoptosis. *Braz. J. Med. Biol. Res.* **2003**, *36* (4), 403−408.
(44) Smidova, A.; Alblova, M.; Kalabova, D.; Psenakova, K.; Rosulek, M.; Herman, P.; Obsil, T.; Obsilova, V. 14−3-3 Protein Masks the Nuclear Localization Sequence of Caspase-2. *FEBS J.* **2018**, *285* (22), 4196−4213.
(45) Jia, H.; Liang, Z.; Zhang, X.; Wang, J.; Xu, W.; Qian, H. 14-3-3 Proteins: An Important Regulator of Autophagy in Diseases. *Am. J. Transl. Res.* **2017**, *9* (11), 4738−4746.
(46) Xing, H.; Zhang, S.; Weinheimer, C.; Kovacs, A.; Muslin, A. J. 14−3-3 Proteins Block Apoptosis and Differentially Regulate MAPK Cascades. *EMBO J.* **2000**, *19* (3), 349−358.
(47) Dong, S.; Kang, S.; Gu, T. L.; Kardar, S.; Fu, H.; Lonial, S.; Khoury, H. J.; Khuri, F.; Chen, J. 14−3-3 Integrates Prosurvival Signals Mediated by the AKT and MAPK Pathways in ZNF198-FGFR1-Transformed Hematopoietic Cells. *Blood* **2007**, *110* (1), 360−369.
(48) Obsilova, V.; Vecer, J.; Herman, P.; Pabianova, A.; Sulc, M.; Teisinger, J.; Boura, E.; Obsil, T. 14−3-3 Protein Interacts with Nuclear Localization Sequence of Forkhead Transcription Factor FoxO4. *Biochemistry* **2005**, *44* (34), 11608−11617.
(49) Silhan, J.; Vacha, P.; Strnadova, P.; Vecer, J.; Herman, P.; Sulc, M.; Teisinger, J.; Obsilova, V.; Obsil, T. 14−3-3 Protein Masks the DNA Binding Interface of Forkhead Transcription Factor FOXO4. *J. Biol. Chem.* **2009**, *284* (29), 19349−19360.
(50) Zanella, F.; dos Santos, N. R.; Link, W. Moving to the Core: Spatiotemporal Analysis of Forkhead Box O (FOXO) and Nuclear Factor-KB (NF-KB) Nuclear Translocation. *Traffic* **2013**, *14* (3), 247−258.
(51) Lin, L.; Hron, J. D.; Peng, S. L. Regulation of NF-KB, Th Activation, and Autoinflammation by the Forkhead Transcription Factor Foxo3a. *Immunity* **2004**, *21* (2), 203−213.
(52) Zhou, W.; Cao, Q.; Peng, Y.; Zhang, Q. J.; Castrillon, D. H.; DePinho, R. A.; Liu, Z. P. FoxO4 Inhibits NF-KB and Protects Mice Against Colonic Injury and Inflammation. *Gastroenterology* **2009**, *137* (4), 1403−1414.
(53) Rodriguez, P. L.; Sahay, S.; Olabisi, O. O.; Whitehead, I. P. ROCK I-Mediated Activation of NF-KB by RhoB. *Cell. Signalling* **2007**, *19* (11), 2361−2369.
(54) Barberan, S.; McNair, K.; Iqbal, K.; Smith, N. C.; Prendergast, G. C.; Stone, T. W.; Cobb, S. R.; Morris, B. J. Altered Apoptotic Responses in Neurons Lacking RhoB GTPase. *Eur. J. Neurosci.* **2011**, *34* (11), 1737−1746.
(55) Sakamoto, K.; Okuwaki, T.; Ushikubo, H.; Mori, A.; Nakahara, T.; Ishii, K. Activation Inhibitors of Nuclear Factor Kappa B Protect Neurons against the NMDA-Induced Damage in the Rat Retina. *J. Pharmacol. Sci.* **2017**, *135* (2), 72−80.
(56) Karatas, H.; Erdener, S. E.; Gursoy-Ozdemir, Y.; Lule, S.; Eren-Kocak, E.; Sen, Z. D.; Dalkara, T. Spreading Depression Triggers Headache by Activating Neuronal Panx1 Channels. *Science (Washington, DC, U. S.)* **2013**, *339* (6123), 1092−1095.
(57) Shi, Y.; Zhang, L.; Teng, J.; Miao, W. *Mol. Med. Rep.* **2018**, 5125−5131.
(58) Palumbo, R.; Galvez, B. G.; Pusterla, T.; De Marchis, F.; Cossu, G.; Marcu, K. B.; Bianchi, M. E. Cells Migrating to Sites of Tissue Damage in Response to the Danger Signal HMGB1 Require NF-KB Activation. *J. Cell Biol.* **2007**, *179* (1), 33−40.
(59) Chen, B.; Liu, J.; Ho, T.-T.; Ding, X.; Mo, Y.-Y. ERK-Mediated NF-KB Activation through ASIC1 in Response to Acidosis. *Oncogenesis* **2016**, *5* (12), No. e279.
(60) Saijo, K.; Mecklenbräuker, I.; Santana, A.; Leitger, M.; Schmedt, C.; Tarakhovsky, A. Protein Kinase C β Controls Nuclear Factor KB Activation in B Cells Through Selective Regulation of the IκB Kinase α. *J. Exp. Med.* **2002**, *195* (12), 1647−1652.
(61) Kim, S. W.; Schifano, M.; Oleksyn, D.; Jordan, C. T.; Ryan, D.; Insel, R.; Zhao, J.; Chen, L. Protein Kinase C-Associated Kinase Regulates NF-KB Activation through Inducing IKK Activation. *Int. J. Oncol.* **2014**, *45* (4), 1707−1714.
(62) Roussos, P.; Katsel, P.; Davis, K. L.; Giakoumaki, S. G.; Siever, L. J.; Bitsios, P.; Haroutunian, V. Convergent Findings for Abnormalities of the NF-KB Signaling Pathway in Schizophrenia. *Neuropsychopharmacology* **2013**, *38* (3), 533−539.
(63) Volk, D. W.; Moroco, A. E.; Roman, K. M.; Edelson, J. R.; Lewis, D. A. The Role of the Nuclear Factor-KB Transcriptional Complex in Cortical Immune Activation in Schizophrenia. *Biol. Psychiatry* **2019**, *85* (1), 25−34.
(64) Ma, H.; Li, B.; Tsien, R. W. Distinct Roles of Multiple Isoforms of CaMKII in Signaling to the Nucleus. *Biochim. Biophys. Acta, Mol. Cell Res.* **2015**, *1853* (9), 1953−1957.
(65) Coyle, J. T. MicroRNAs Suggest a New Mechanism for Altered Brain Gene Expression in Schizophrenia. *Proc. Natl. Acad. Sci. U. S. A.* **2009**, *106* (9), 2975−2976.
(66) Ma, H.; Groth, R. D.; Cohen, S. M.; Emery, J. F.; Li, B.; Hoedt, E.; Zhang, G.; Neubert, T. A.; Tsien, R. W. ΓcaMKII Shuttles Ca 2+ /CaM to the Nucleus to Trigger CREB Phosphorylation and Gene Expression. *Cell* **2014**, *159* (2), 281−294.
(67) Cohen, S. M.; Suutari, B.; He, X.; Wang, Y.; Sanchez, S.; Tirko, N. N.; Mandelberg, N. J.; Mullins, C.; Zhou, G.; Wang, S.; et al. Calmodulin Shuttling Mediates Cytonuclear Signaling to Trigger Experience-Dependent Transcription and Memory. *Nat. Commun.* **2018**, *9* (1), 1−12.
(68) Saura, C. A.; Valero, J. The Role of CREB Signaling in Alzheimer's Disease and Other Cognitive Disorders. *Rev. Neurosci.* **2011**, *22* (2), 153−169.
(69) Graham, J. M. Preparation of Crude Subcellular Fractions by Differential Centrifugation. *Sci. World J.* **2002**, *2*, 1638−1642.
(70) Collins, T. J. Mitochondria Are Morphologically Heterogeneous within Cells. *J. Exp. Biol.* **2003**, *206* (12), 1993−2000.
(71) Kuznetsov, A. V.; Troppmair, J.; Sucher, R.; Hermann, M.; Saks, V.; Margreiter, R. Mitochondrial Subpopulations and Heterogeneity Revealed by Confocal Imaging: Possible Physiological Role? *Biochim. Biophys. Acta, Bioenerg.* **2006**, *1757* (5−6), 686−691.
(72) Brown, M. R.; Sullivan, P. G.; Geddes, J. W. Synaptic Mitochondria Are More Susceptible to Ca2+ Overload than Nonsynaptic Mitochondria. *J. Biol. Chem.* **2006**, *281* (17), 11658−11668.

DOI: 10.1021/acs.jproteome.9b00398
J. Proteome Res. XXXX, XXX, XXX−XXX

(73) Kuznetsov, A. V.; Margreiter, R. Heterogeneity of Mitochondria and Mitochondrial Function within Cells as Another Level of Mitochondrial Complexity. *Int. J. Mol. Sci.* **2009**, *10* (4), 1911−1929.
(74) Woods, D. C. Mitochondrial Heterogeneity: Evaluating Mitochondrial Subpopulation Dynamics in Stem Cells. *Stem Cells Int.* **2017**, *2017*, 7068567.
(75) Rollins, B. L.; Morgan, L.; Hjelm, B. E.; Sequeira, A.; Schatzberg, A. F.; Barchas, J. D.; Lee, F. S.; Myers, R. M.; Watson, S. J.; Akil, H.; et al. Mitochondrial Complex I Deficiency in Schizophrenia and Bipolar Disorder and Medication Influence. *Mol. Neuropsychiatry* **2018**, *3* (3), 157−169.
(76) Holper, L.; Ben-Shachar, D.; Mann, J. Multivariate Meta-Analyses of Mitochondrial Complex I and IV in Major Depressive Disorder, Bipolar Disorder, Schizophrenia, Alzheimer Disease, and Parkinson Disease. *Neuropsychopharmacology* **2019**, *44* (5), 837−849.
(77) Akarsu, S.; Torun, D.; Bolu, A.; Erdem, M.; Kozan, S.; Ak, M.; Akar, H.; Uzun, Ö. Mitochondrial Complex I and III Gene MRNA Levels in Schizophrenia, and Their Relationship with Clinical Features. *J. Mol. psychiatry* **2014**, *2* (1), 6.
(78) Farinelli, S. E.; Nicklas, W. J. Glutamate Metabolism in Rat Cortical Astrocyte Cultures. *J. Neurochem.* **1992**, *58* (5), 1905−1915.
(79) Hassel, B.ør.; Bachelard, H.; Jones, P.; Fonnum, F.; Sonnewald, U. Trafficking of Amino Acids between Neurons and Glia In Vivo. Effects of Inhibition of Glial Metabolism by Fluoroacetate. *J. Cereb. Blood Flow Metab.* **1997**, *17*, 1230−1238.
(80) Poels, E. M. P.; Kegeles, L. S.; Kantrowitz, J. T.; Slifstein, M.; Javitt, D. C.; Lieberman, J. A.; Abi-Dargham, A.; Girgis, R. R. Imaging Glutamate in Schizophrenia: Review of Findings and Implications for Drug Discovery. *Mol. Psychiatry* **2014**, *19* (1), 20−29.
(81) Bruneau, E. G.; McCullumsmith, R. E.; Haroutunian, V.; Davis, K. L.; Meador-Woodruff, J. H. Increased Expression of Glutaminase and Glutamine Synthetase MRNA in the Thalamus in Schizophrenia. *Schizophr. Res.* **2005**, *75* (1), 27−34.
(82) Boksha, I. S.; Tereshkina, E. B.; Savushkina, O. K.; Prokhorova, T. A.; Vorobyeva, E. A.; Burbaeva, G. S. Comparative Studies of Glutamine Synthetase Levels in the Brains of Patients with Schizophrenia and Mentally Healthy People. *Neurochem. J.* **2018**, *12* (1), 95−101.
(83) Burbaeva, G. S.; Boksha, I. S.; Turishcheva, M. S.; Vorobyeva, E. A.; Savushkina, O. K.; Tereshkina, E. B. Glutamine Synthetase and Glutamate Dehydrogenase in the Prefrontal Cortex of Patients with Schizophrenia. *Prog. Neuro-Psychopharmacol. Biol. Psychiatry* **2003**, *27* (4), 675−680.
(84) Prokhorova, T. A.; Boksha, I. S.; Savushkina, O. K.; Tereshkina, E. B.; Vorobyeva, E. A.; Pomytkin, A. N.; Kaleda, V. G.; Burbaeva, G. S. Glutamate Dehydrogenase Activity in Platelets of Patients with Endogenous Psychosis. *Zhurnal Nevrol. i psikhiatrii im. S.S. Korsakova* **2016**, *116* (3), 44.
(85) Lander, S. S.; Khan, U.; Lewandowski, N.; Chakraborty, D.; Provenzano, F. A.; Mingote, S.; Chornyy, S.; Frigerio, F.; Maechler, P.; Kaphzan, H.; et al. Glutamate Dehydrogenase-Deficient Mice Display Schizophrenia-Like Behavioral Abnormalities and CA1-Specific Hippocampal Dysfunction. *Schizophr. Bull.* **2019**, *45* (1), 127−137.
(86) Desilva, T. M.; Borenstein, N. S.; Volpe, J. J.; Kinney, H. C.; Rosenberg, P. A. Expression of EAAT2 in Neurons and Protoplasmic Astrocytes during Human Cortical Development. *J. Comp. Neurol.* **2012**, *520* (17), 3912−3932.
(87) Parkin, G. M.; Udawela, M.; Gibbons, A.; Dean, B. Glutamate Transporters, EAAT1 and EAAT2, Are Potentially Important in the Pathophysiology and Treatment of Schizophrenia and Affective Disorders. *World J. Psychiatry* **2018**, *8* (2), 51−63.
(88) Bauer, D.; Gupta, D.; Harotunian, V.; Meador-Woodruff, J. H.; McCullumsmith, R. E. Abnormal Expression of Glutamate Transporter and Transporter Interacting Molecules in Prefrontal Cortex in Elderly Patients with Schizophrenia. *Schizophr Res.* **2008**, *104* (1−3), 108−120.
(89) Matute, C.; Melone, M.; Vallejo-Illarramendi, A.; Conti, F. Increased Expression of the Astrocytic Glutamate Transporter GLT-1 in the Prefrontal Cortex of Schizophrenics. *Glia* **2005**, *49* (3), 451−455.
(90) McCullumsmith, R. E.; O'Donovan, S. M.; Drummond, J. B.; Benesh, F. S.; Simmons, M.; Roberts, R.; Lauriat, T.; Haroutunian, V.; Meador-Woodruff, J. H. Cell-Specific Abnormalities of Glutamate Transporters in Schizophrenia: Sick Astrocytes and Compensating Relay Neurons? *Mol. Psychiatry* **2016**, *21* (6), 823−830.
(91) Farkas, I.; Baranyi, L.; Ishikawa, Y.; Okada, N.; Bohata, C.; Budai, D.; Fukuda, A.; Imai, M.; Okada, H. CD59 Blocks Not Only the Insertion of C9 into MAC but Inhibits Ion Channel Formation by Homologous C5b-8 as Well as C5b-9. *J. Physiol.* **2002**, *539* (2), 537−545.
(92) Yasojima, K.; McGeer, E. G.; McGeer, P. L. Complement Regulators C1 Inhibitor and CD59 Do Not Significantly Inhibit Complement Activation in Alzheimer Disease. *Brain Res.* **1999**, *833* (2), 297−301.
(93) Lian, H.; Yang, L.; Cole, A.; Sun, L.; Chiang, A. C.-A.; Fowler, S. W.; Shim, D. J.; Rodriguez-Rivera, J.; Taglialatela, G.; Jankowsky, J. L.; Lu, H.-C.; Zheng, H. NFκB-Activated Astroglial Release of Complement C3 Compromises Neuronal Morphology and Function Associated with Alzheimer's Disease. *Neuron* **2015**, *85* (1), 101−115.
(94) Stephan, A. H.; Barres, B. A.; Stevens, B. The Complement System: An Unexpected Role in Synaptic Pruning During Development and Disease. *Annu. Rev. Neurosci.* **2012**, *35* (1), 369−389.
(95) Presumey, J.; Bialas, A. R.; Carroll, M. C. Complement System in Neural Synapse Elimination in Development and Disease. *Adv. Immunol.* **2017**, *135*, 53−79.
(96) Li, Z.; Jo, J.; Jia, J.-M.; Lo, S.-C.; Whitcomb, D. J.; Jiao, S.; Cho, K.; Sheng, M. Caspase-3 Activation via Mitochondria Is Required for Long-Term Depression and AMPA Receptor Internalization. *Cell* **2010**, *141* (5), 859−871.
(97) Sekar, A.; Bialas, A. R.; De Rivera, H.; Davis, A.; Hammond, T. R.; Kamitaki, N.; Tooley, K.; Presumey, J.; Baum, M.; Van Doren, V.; et al. Schizophrenia Risk from Complex Variation of Complement Component 4. *Nature* **2016**, *530* (7589), 177−183.
(98) Holahan, M. GAP-43 in Synaptic Plasticity: Molecular Perspectives. *Res. Rep. Biochem.* **2015**, 137.
(99) Chambers, J. S.; Thomas, D.; Saland, L.; Neve, R. L.; Perrone-Bizzozero, N. I. Growth-Associated Protein 43 (GAP-43) and Synaptophysin Alterations in the Dentate Gyrus of Patients with Schizophrenia. *Prog. Neuro-Psychopharmacol. Biol. Psychiatry* **2005**, *29* (2), 283−290.
(100) Hung, C.-C.; Lin, C.-H.; Chang, H.; Wang, C.-Y.; Lin, S.-H.; Hsu, P.-C.; Sun, Y.-Y.; Lin, T.-N.; Shie, F.-S.; Kao, L.-S.; et al. Astrocytic GAP43 Induced by the TLR4/NF-KB/STAT3 Axis Attenuates Astrogliosis-Mediated Microglial Activation and Neurotoxicity. *J. Neurosci.* **2016**, *36* (6), 2027−2043.
(101) Jung, H.; Yoon, B. C.; Holt, C. E. Axonal MRNA Localization and Local Protein Synthesis in Nervous System Assembly, Maintenance and Repair. *Nat. Rev. Neurosci.* **2012**, *13* (5), 308−324.
(102) Doudna, J. A; Rath, V. L Structure and Function of the Eukaryotic Ribosome: The Next Frontier. *Cell* **2002**, *109* (2), 153−156.
(103) Buffington, S. A.; Huang, W.; Costa-Mattioli, M. Translational Control in Synaptic Plasticity and Cognitive Dysfunction. *Annu. Rev. Neurosci.* **2014**, *37*, 17−38.
(104) English, J. A.; Fan, Y.; Föcking, M.; Lopez, L. M.; Hryniewiecka, M.; Wynne, K.; Dicker, P.; Matigian, N.; Cagney, G.; Mackay-Sim, A.; et al. Reduced Protein Synthesis in Schizophrenia Patient-Derived Olfactory Cells. *Transl. Psychiatry* **2015**, *5* (April), No. e663.
(105) Zhou, X.; Liao, W.-J.; Liao, J.-M.; Liao, P.; Lu, H. Ribosomal Proteins: Functions beyond the Ribosome. *J. Mol. Cell Biol.* **2015**, *7* (2), 92−104.
(106) Filip, A. M.; Klug, J.; Cayli, S.; Fröhlich, S.; Henke, T.; Lacher, P.; Eickhoff, R.; Bulau, P.; Linder, M.; Carlsson-Skwirut, C.; et al. Ribosomal Protein S19 Interacts with Macrophage Migration Inhibitory Factor and Attenuates Its Pro-Inflammatory Function. *J. Biol. Chem.* **2009**, *284* (12), 7977−7985.

DOI: 10.1021/acs.jproteome.9b00398
J. Proteome Res. XXXX, XXX, XXX−XXX

(107) Lv, J.; Huang, X. R.; Klug, J.; Fröhlich, S.; Lacher, P.; Xu, A.; Meinhardt, A.; Lan, H. Y. Ribosomal Protein S19 Is a Novel Therapeutic Agent in Inflammatory Kidney Disease. *Clin. Sci.* **2013**, *124* (10), 627−637.
(108) Zhang, S.; Zis, O.; Ly, P. T. T.; Wu, Y.; Zhang, S.; Zhang, M.; Cai, F.; Bucala, R.; Shyu, W. C.; Song, W. Down-Regulation of MIF by NFκB under Hypoxia Accelerated Neuronal Loss during Stroke. *FASEB J.* **2014**, *28* (10), 4394−4407.
(109) Jin, A.; Itahana, K.; O'Keefe, K.; Zhang, Y. Inhibition of HDM2 and Activation of P53 by Ribosomal Protein L23. *Mol. Cell. Biol.* **2004**, *24* (17), 7669−7680.
(110) Wanzel, M.; Russ, A. C.; Kleine-Kohlbrecher, D.; Colombo, E.; Pelicci, P. G.; Eilers, M. A Ribosomal Protein L23-Nucleophosmin Circuit Coordinates Miz1 Function with Cell Growth. *Nat. Cell Biol.* **2008**, *10* (9), 1051−1061.
(111) Yang, L.; Zhu, J.-y.; Zhang, J.-g.; Bao, B.-j.; Guan, C.-q.; Yang, X.-j.; Liu, Y.-h.; Huang, Y.-j.; Ni, R.-z.; Ji, L.-l. Far Upstream Element-Binding Protein 1 (FUBP1) Is a Potential c-Myc Regulator in Esophageal Squamous Cell Carcinoma (ESCC) and Its Expression Promotes ESCC Progression. *Tumor Biol.* **2016**, *37* (3), 4115−4126.
(112) Duan, J.; Bao, X.; Ma, X.; Zhang, Y.; Ni, D.; Wang, H.; Zhang, F.; Du, Q.; Fan, Y.; Chen, J.; et al. Upregulation of Far Upstream Element-Binding Protein 1 (FUBP1) Promotes Tumor Proliferation and Tumorigenesis of Clear Cell Renal Cell Carcinoma. *PLoS One* **2017**, *12* (1), e0169852.
(113) Dang, C. V. C-Myc Target Genes Involved in Cell Growth, Apoptosis, and Metabolism. *Mol. Cell. Biol.* **1999**, *19* (1), 1−11.
(114) Lee, H. G.; Casadesus, G.; Nunomura, A.; Zhu, X.; Castellani, R. J.; Richardson, S. L.; Perry, G.; Felsher, D. W.; Petersen, R. B.; Smith, M. A. The Neuronal Expression of MYC Causes a Neurodegenerative Phenotype in a Novel Transgenic Mouse. *Am. J. Pathol.* **2009**, *174* (3), 891−897.
(115) Lee, H.-P.; Kudo, W.; Zhu, X.; Smith, M. A.; Lee, H.-g. Early Induction of C-Myc Is Associated with Neuronal Cell Death. *Neurosci. Lett.* **2011**, *505* (2), 124−127.
(116) Qin, Z. H.; Chen, R. W.; Wang, Y.; Nakai, M.; Chuang, D. M.; Chase, T. N. Nuclear Factor KappaB Nuclear Translocation Upregulates C-Myc and P53 Expression during NMDA Receptor-Mediated Apoptosis in Rat Striatum. *J. Neurosci.* **1999**, *19* (10), 4023−4033.
(117) Herold, S.; Wanzel, M.; Beuger, V.; Frohme, C.; Beul, D.; Hillukkala, T.; Syvaoja, J.; Saluz, H. P.; Haenel, F.; Eilers, M. Negative Regulation of the Mammalian UV Response by Myc through Association with Miz-1. *Mol. Cell* **2002**, *10* (3), 509−521.
(118) Qi, Y.; Li, X.; Chang, C.; Xu, F.; He, Q.; Zhao, Y.; Wu, L. Ribosomal Protein L23 Negatively Regulates Cellular Apoptosis via the RPL23/Miz-1/c-Myc Circuit in Higher-Risk Myelodysplastic Syndrome. *Sci. Rep.* **2017**, *7* (1), 1−12.
(119) Patel, J. H.; McMahon, S. B. Targeting of Miz-1 Is Essential for Myc-Mediated Apoptosis. *J. Biol. Chem.* **2006**, *281* (6), 3283−3289.
(120) Wolf, E.; Gebhardt, A.; Kawauchi, D.; Walz, S.; von Eyss, B.; Wagner, N.; Renninger, C.; Krohne, G.; Asan, E.; Roussel, M. F.; Eilers, M. Miz1 is required to maintain autophagic flux. *Nat. Commun.* **2013**, *4*, 2535.
(121) Kleiger, G.; Mayor, T. Perilous Journey: A Tour of the Ubiquitin-Proteasome System. *Trends Cell Biol.* **2014**, *24* (6), 352−359.
(122) Hsu, M. T.; Guo, C. L.; Liou, A. Y.; Chang, T. Y.; Ng, M. C.; Florea, B. I.; Overkleeft, H. S.; Wu, Y. L.; Liao, J. C.; Cheng, P. L. Stage-Dependent Axon Transport of Proteasomes Contributes to Axon Development. *Dev. Cell* **2015**, *35* (4), 418−431.
(123) Altar, C. A.; Jurata, L. W.; Charles, V.; Lemire, A.; Liu, P.; Bukhman, Y.; Young, T. A.; Bullard, J.; Yokoe, H.; Webster, M. J.; et al. Deficient Hippocampal Neuron Expression of Proteasome, Ubiquitin, and Mitochondrial Genes in Multiple Schizophrenia Cohorts. *Biol. Psychiatry* **2005**, *58* (2), 85−96.
(124) Rubio, M. D.; Wood, K.; Haroutunian, V.; Meador-Woodruff, J. H. Dysfunction of the Ubiquitin Proteasome and Ubiquitin-Like Systems in Schizophrenia. *Neuropsychopharmacology* **2013**, *38* (10), 1910−1920.
(125) Haroon, E.; Miller, A. H.; Sanacora, G. Inflammation, Glutamate, and Glia: A Trio of Trouble in Mood Disorders. *Neuropsychopharmacology* **2017**, *42* (1), 193−215.
(126) Guerrini, L.; Blasi, F.; Denis-Donini, S. Synaptic Activation of NF-Kappa B by Glutamate in Cerebellar Granule Neurons in Vitro. *Proc. Natl. Acad. Sci. U. S. A.* **1995**, *92*, 9077−9081.
(127) Homayoun, H.; Moghaddam, B. Orbitofrontal Cortex Neurons as a Common Target for Classic and Glutamatergic Antipsychotic Drugs. *Proc. Natl. Acad. Sci. U. S. A.* **2008**, *105* (46), 18041−18046.
(128) Dai, M.-S.; Zeng, S. X.; Jin, Y.; Sun, X.-X.; David, L.; Lu, H. Ribosomal Protein L23 Activates P53 by Inhibiting MDM2 Function in Response to Ribosomal Perturbation but Not to Translation Inhibition. *Mol. Cell. Biol.* **2004**, *24* (17), 7654−7668.
(129) Clasen, S. J.; Shao, W.; Gu, H.; Espenshade, P. J. Prolyl Dihydroxylation of Unassembled US12/Rps23 Regulates Fungal Hypoxic Adaptation. *eLife* **2017**, *6*, 1−29.

DOI: 10.1021/acs.jproteome.9b00398
J. Proteome Res. XXXX, XXX, XXX−XXX